INFLUENCE OF MICROSTRUCTURE AND MOIST ENVIRONMENT ON FATIGUE CRACK PROPAGATION IN METALLIC ALLOYS

JEAN PETIT

An overview on some aspects of the role of microstructure and of moist environment on fatigue crack propagation is given. The respective influence of several microstructural parameters as grain size, texture, alloy phases, ageing conditions, and of extrinsic factors as crack closure and environment for metallic alloys is illustrated and discussed.

1. Introduction

Defect tolerance design approach to fatigue is based on the premise that engineering structures are inherently flawed. Then, the useful fatigue life is the number of cycles to propagate a dominant flaw of an assumed or measured initial size (which can be the largest undetected crack size estimated from the sensitivity of non-destructive inspection methods) to a critical dimension which may be dictated by the fracture toughness, limit load, allowable strain, or allowable compliance change. In most metallic materials, catastrophic failure is preceded by a substantial amount of stable crack growth under cyclic loading conditions. The propagation rate of these cracks for given loading conditions depends on several factors including crack length and geometry of the cracked structure, crack closure, temperature, environment, test frequency and propagation mechanisms in relation with material microstructure. Indeed the fatigue fracture behaviour of metals and metallic alloys has been shown widely influenced by material composition and by various microstructural parameters. Numerous articles can be found in the literature on these topics. Some excellent reviews can be mentioned [1–3] but it would be a task beyond the scope of this paper to refer to all of them.

In this overview a selection of demonstrative examples provided by the literature and the works of the present authors will give illustrations of the respective role of grain size, texture, alloy phases, and age-hardening. In comparison to the intrinsic propagation behaviour characterized under inert environment and after

Prof. J. Petit, Laboratoire de Mécanique et de Physique des Matériaux, UMR CNRS N° 6617, ENSMA, Téléport 2, BP. 109, 86960 FUTUROSCOPE Cedex, France.

crack closure correction, an evaluation is made of the role of two dominant extrinsic parameters, i.e. environment and crack closure, since they can deeply affect the fatigue behaviour in different ways [4].

2. Influence of microstructural parameters

2.1 Grain size

Grains boundaries can constitute high obstacle to the movement of dislocations, thus increasing the flow stress according to the Hall-Petch relation. Fatigue process, being basically the result of cumulated plastic deformation, can be affected by hardening processes, and can also interact with grain boundaries. Numerous studies have shown that the decrease of grain size improves the fatigue limit but conversely reduces the resistance against the crack propagation. Recently, Haberz et al. [5] have clearly demonstrated in ARMCO iron with different grain sizes ranging between 3 and 3000 μm that the nominal stress intensity threshold is strongly influenced by the grain size (Fig. 1). But after correction for closure, the effective threshold is not significantly affected. Consequently, the change of the threshold is mainly caused by the increase of the roughness induced closure effect [6, 7] with increasing grain size. Such observations are in accordance with many others, but the range of grain size explored here is exceptional. Finally, it comes out from this work that there is no substantial influence of grain size on the effective behaviour of a stage II crack. But when the near-threshold propagation is characterized by a strong localization of the plastic deformation [8, 9], the resulting crack growth behaviour can be strongly affected by the microstructure even after closure correction as illustrated in Fig. 2 for a Ti-6Al-4V alloy in different thermo-mechanical conditions.

2.2 Texture

The texture can modify the nominal crack propagation ($R = 0.1$ in air) as illustrated in Fig. 3 for a 2090 – T8X aluminium lithium alloy [10]. Faster crack growth and lower threshold are observed in the 1.6 mm T83 thin sheet compared to the 12.7 mm T81 thick plate for tests performed in the LT orientation. But after closure correction both materials present the same effective behaviour. The more zig-zagging crack path in the thick plate only increases the contribution of the roughness induced closure (or non-closure) as illustrated in Fig. 3, but does not affect the crack growth mechanism in itself.

2.3 Alloy phases

Two examples have been selected to illustrate the influence of alloy phases on crack propagation. Data in duplex (iced water quenched after 1 h/760 °C)

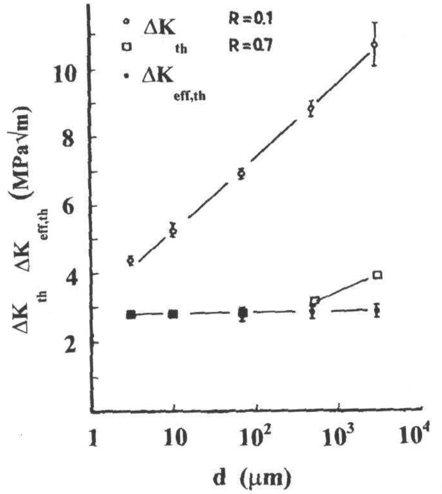

Fig. 1. Threshold and effective threshold as functions of the grain size in ARMCO steel (Haberz et al., 1993).

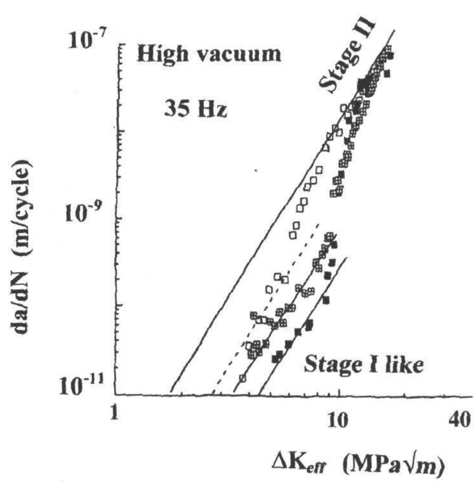

Fig. 2. Intrinsic fatigue crack propagation Ti-6Al-4V at 300 °C: □ – bimodal 40% α_p ($\phi = 20\ \mu$m), ⊞ – globular 80% α_p ($\phi = 8\ \mu$m + lamellae of 50 μm), ■ – globular 75% α_p ($\phi = 8\ \mu$m).

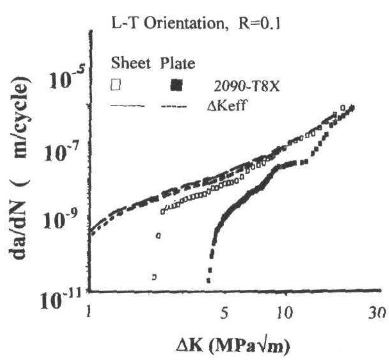

Fig. 3. Fatigue crack propagation in 1.6 mm-thin sheet and 12.7 mm-thick plate of 2090 T8X Al-Li alloy (Vankateswara et al., 1991).

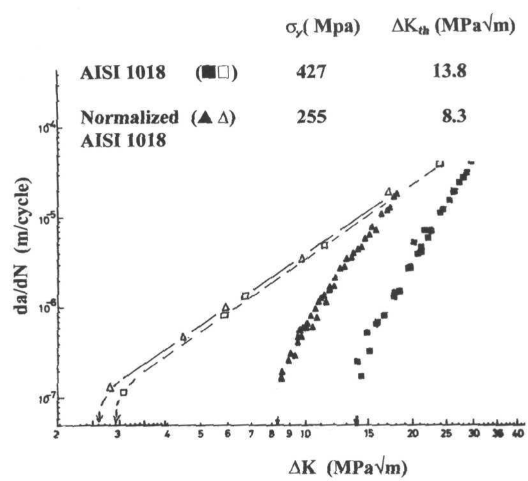

Fig. 4. Rate of growth vs. ΔK for AISI 1018 in Duplex and normalized conditions. Effective data (open symbols) are plotted using crack opening measurements from Minakawa et al., 1982.

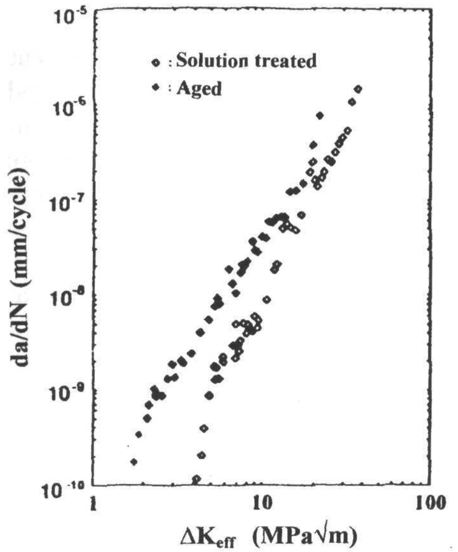

Fig. 5. Relations between da/dN and ΔK_{eff} in solution treated specimen and aged specimen of Ti-6Al-2Sn-4Zr-6Mo forged bars (Niinomi et al., 1993).

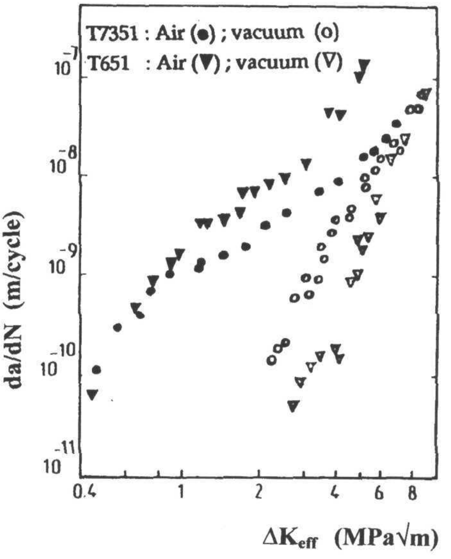

Fig. 6. Illustration of interaction between microstructure and environment on a 7075 alloy in two ageing conditions tested in ambient air and high vacuum.

and normalized AISI-1018 are plotted in Fig. 4 [11]. Obviously, the resistance of the duplex structure against crack propagation for a fatigue test performed at a R ratio of 0.05 is very much higher than that of the normalized material. It could be attractive to relate such performance and high threshold level to the increase in the yield stress (427 MPa and 255 MPa for duplex and normalized conditions, respectively). But after closure correction, the effective propagation of both microstructures is identical. Hence the differences in the nominal curves must be attributed to the difference existing in the contribution of crack closure. Here again the microstructure does not affect the effective stage II propagation.

The next example (Fig. 5) shows the effect of retained metastable β phase on fatigue crack propagation characteristics of forged bars of a Ti 6246 titanium alloy. The crack propagation rates in the aged material (6 h at 863 K of solutionizing) are substantially lower than in the as-solutionized microstructure, with a threshold range decreased of more than 50%. In this case, even after closure correction, there is still a large difference between the two microstructures. This example shows that when the propagation mechanism in itself is changed from one microstructure to the other, the effective behaviour is also modified.

2.4 Aged conditions

An illustration of the coupled influence of microstructure and environment still existing after closure correction is given in Fig. 6 on a 7075 alloy in two aged conditions tested in ambient air and high vacuum [4]. The peak-aged matrix contains shareable Guinier-Preston zones and shareable precipitates which promote a localization of the plastic deformation within a single slip system in each individual grain along the crack front. The over-aged matrix contains larger and less coherent precipitates which favour a wavy slip mechanism [4, 12, 13]. In vacuum, the peak-aged T651 condition leads to a highly retarded crystallographic propagation (so called stage-I-like regime) while the over-aged T7351 condition gives a conventional stage II propagation. In ambient air, the single slip mechanism which is still operative in the peak-aged alloy, is assumed to offer a preferential path for hydrogen embrittlement which leads to a strongly accelerated propagation. Conversely ambient air has little influence on the stage II regime as observed in the over-aged alloy. It can be noticed that the influence of ambient air has inverted the ranking of the propagation curves with respect to the microstructures. It can be underlined that a crystallographic propagation is faster than stage II in air, but is highly retarded in vacuum. These results indicate a high sensitivity of the slip mechanisms to environment, specially near the grain boundaries, and hence a large influence of environment on the microstructural barrier effects.

3. Intrinsic fatigue crack growth

The above examples have shown that if one intends to analyze the specific role of microstructure it would be useful to analyze the crack propagation behaviour of the material in conditions where the influence of crack closure and environment are eliminated, that is to say, to examine the intrinsic fatigue-crack-growth behaviour.

On the basis of numerous experimental data obtained in high vacuum on technical aluminium alloys with various ageing conditions, on aluminium based single crystals and on steels and titanium alloys, it has been shown [4] that the intrinsic fatigue crack growth can be described according to three characteristic regimes (see example of Al alloys in Fig. 7):

– The faster intrinsic stage I has been identified on single crystals of Al-Zn-Mg alloys [4] with a peak-aged microstructure which favours crystallographic propagation along a PSB (persistent slip bands) which develop in {111} planes pre-oriented for single slip. This regime is also observed on various materials in the early growth of microstructural short cracks [14]).

– The intermediate intrinsic stage II is commonly observed on polycrystals and single crystals when crack propagation proceeds at macroscopic scale along planes normal to the loading direction. Such propagation is induced by microstructures which promote homogeneous deformation and wavy slip as large or non-coherent

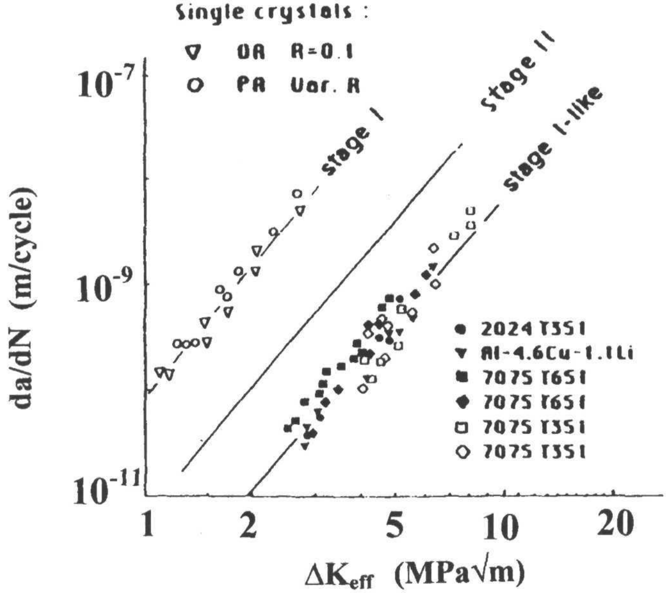

Fig. 7. Illustration of the three intrinsic propagation regimes for Al alloys.

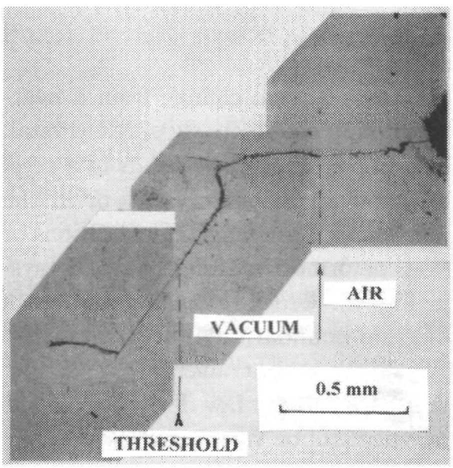

Fig. 8. Stage I to stage II transition in a peak aged single crystal of Al-4.5% Zn-12.5% Mg pre-oriented for single slip (high vacuum, $R = 0.1$, 35 Hz).

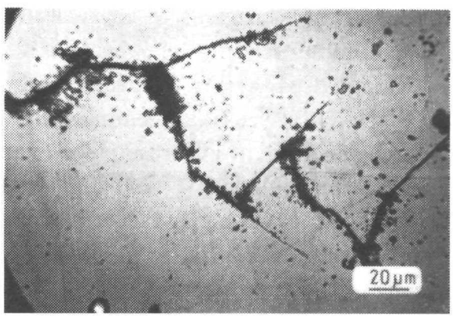

Fig. 9. Stage I-like propagation in 2024T351 tested in high vacuum ($R = 0.5$, $da/dN = 2 \times 10^{-11}$ m/cycle).

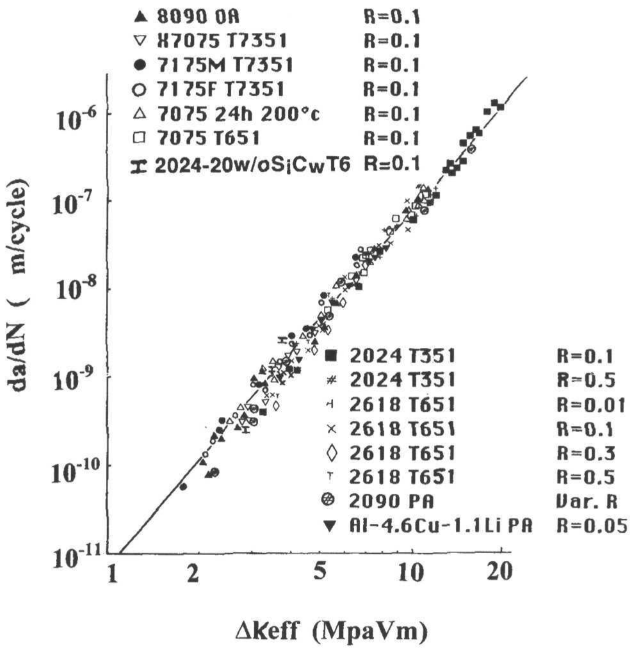

Fig. 10. Intrinsic stage II propagation. Al-based alloys.

precipitates or small grains size. Fig. 8 illustrates a typical change from a near--threshold stage I to a mid-ΔK stage II propagation in an Al-Zn-Mg single crystal.

The slowest regime, or intrinsic stage-I-like propagation corresponds to a crystallographic crack growth observed near the threshold in polycrystals or in the early stage of growth of naturally initiated micro-cracks, when ageing conditions or low stacking fault energy generate heterogeneous deformation along single slip systems within individual grains (see example in Fig. 9). Crack branching and crack deviation mechanisms [7] and barrier effect of grain boundaries [4] are assumed to lower the stress intensity factor at the crack tip of the main crack.

The stage II regime is in accordance with a propagation law derived from the models initially proposed by Mc Clintock [15], Rice [16] or Weertman [17]:

$$\mathrm{d}a/\mathrm{d}N = A/D^*(\Delta K_{\mathrm{eff}}/\mu)^4, \tag{1}$$

where A is the dimensionless parameter, μ the shear modulus, and D^* the critical cumulated displacement leading to a rupture over a crack increment ahead of the crack tip.

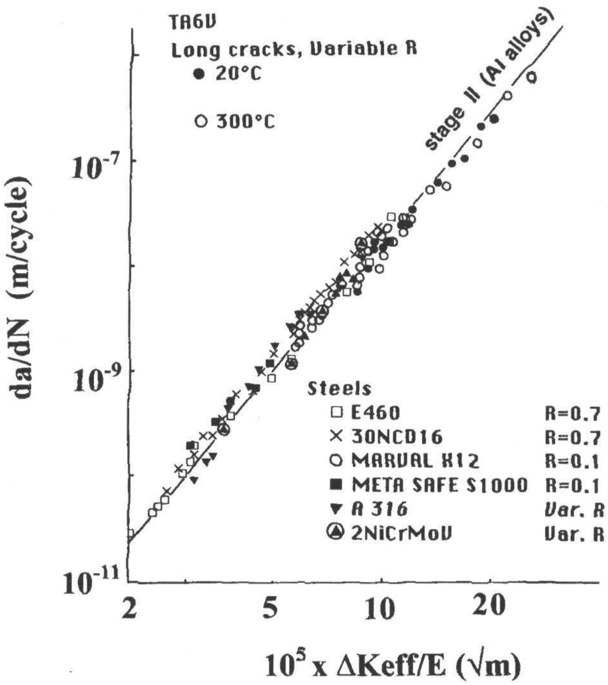

Fig. 11. Intrinsic stage II propagation. Steels and TA6V alloy compared to mean curves for Al alloys after rationalization in terms of $\Delta K_{\text{eff}}/E$.

Intrinsic data for well identified stage II propagation are plotted in Fig. 10 in a $\mathrm{d}a/\mathrm{d}N$ vs. $\Delta K_{\text{eff}}/E$ (E – Young Modulus) diagram for a wide selection of Al alloys, and in Fig. 11 for a selection of steels and a TA6V Ti alloy compared to the mean curve for Al alloys. This diagram constitutes an excellent validation of the above relation and confirms that the LEFM concept is very well adapted to describe the intrinsic growth of a stage II crack which clearly appears to be nearly independent on the alloy composition, the microstructure (when it does not introduce a change in the deformation mechanism), the grain size, and, hence, the yield stress. The predominant factor is the Young modulus of the matrix, and the slight differences existing between the three base metals can be interpreted as some limited change in D^* according to the alloy ductility [4].

The stage-I-like regime cannot be rationalized using the above relation (Figs. 2 and 12). The retardation is highly sensitive to the microstructure; it is well marked when the number of available slip systems is limited (Ti alloys) or can be nearly absent when some secondary slip systems can be activated near the boundaries as observed in Al-Li alloys [18].

4. Environmentally assisted propagation

Following the rationalization of intrinsic stage II propagation as presented above, some similar rationalization of FCG in air could be expected after correction for crack closure and temperature effects ($\Delta K_{\text{eff}}/E$). Fig. 13 presents a compilation of stage-II-propagation data obtained in ambient air for almost the same alloys as in vacuum (see Figs. 10 and 11). Obviously rationalization does not exist in air. The sensitivity to air environment is shown strongly dependent as well on base metals, addition elements, and microstructures (see 7075 alloy in three different conditions) as on the R ratio and the growth-rate range. However a typical common critical rate range can be pointed out at about 10^{-8} m/cycle for all materials. This critical step is associated to stress intensity factor ranges at which the plastic zone size at the crack tip is of the same order as grain or sub-grain diameters. In addition there is a general agreement to consider that, for growth rates lower than this critical range, crack propagation results from a step-by-step advance mechanism instead of a cycle-by-cycle progression as generally observed in the Paris regime in air.

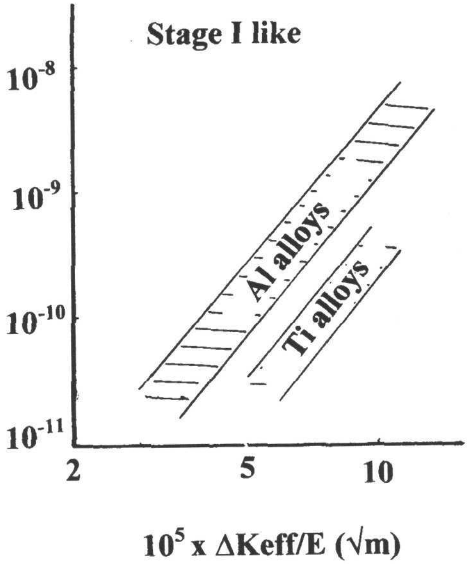

Fig. 12. Comparison of intrinsic stage I-like propagation for Al alloys and TA6V alloys in the $\mathrm{d}a/\mathrm{d}N$ vs. $\Delta K_{\text{eff}}/E$ diagram.

A comprehensive model has been established for environmentally assisted crack growth [4, 8, 19] as schematically illustrated in Fig. 14:

– at growth rates higher than a critical rate $(\mathrm{d}a/\mathrm{d}N)_{cr}$ which depends upon several factors as surrounding partial pressure of water vapour, load ratio, test frequency, chemical composition and microstructure, the crack-growth mechanism is assisted by water vapour adsorption but it is still controlled by plasticity as in vacuum.

– at growth rates lower than $(\mathrm{d}a/\mathrm{d}N)_{cr}$, hydrogen-assisted crack-growth mechanism becomes operative, hydrogen being provided by adsorbed water vapour when some critical conditions are fulfilled.

At room temperature and for conventional test frequencies of 20 to 50 Hz, $(\mathrm{d}a/\mathrm{d}N)_{cr}$ is about 10^{-8} m/cycle as pointed out in Fig. 15. As recently described [19], the adsorption-assisted stage II propagation verify relation (1), adsorption

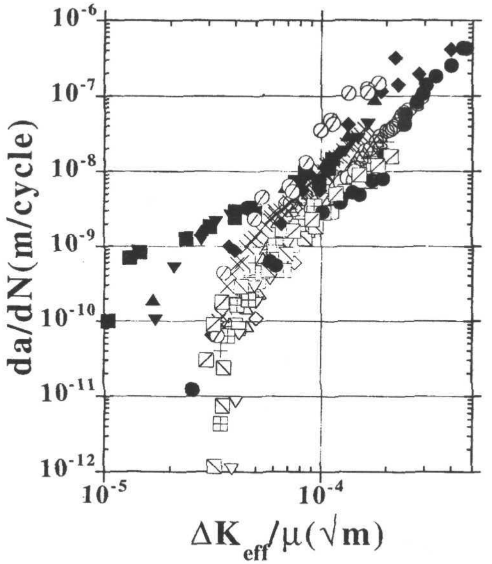

Steels		Al-alloys	
o MARVAL X12 METASAFE ◊ 2NiCrMoV [125] x 30NCD16 + E460 ⊡ 316L	▿ 3044 [127] ▵ low-carbon steel ambient air [126] ⊖ low-carbon steel dry air [126] ⊞ 403 [127] ⧅ 430 [127]	♦ 2024 R = 0.1 ● 2024 P = 0.5 ▲ 7175F T7351 ▼ 7175M T7351	■ X7175 T7351 ⌀ 7075 T7351 ⧄ 3Li R = 0.5

Fig. 13. Effective data in terms of $(\Delta K_{\text{eff}}/\mu)$ (μ = shear modulus) for steels and Al alloys.

being just assumed to reduce the cumulated displacement D^* in accordance with Lynch approach [20]. The modelling of the hydrogen-assisted propagation has to be developed by the introduction of the coupled effect of two concurrent mechanisms, i.e. hydrogen action and plastic cyclic accumulation, which can be strongly affected by environment and temperature. Up to now no fatigue-crack-growth law is available which takes into account the different processes described above. Theoretical models do not account for environmental effects and therefore they are merely valid for fatigue crack propagation in inert atmospheres. Similarly, fatigue-crack-growth laws considering the strained material at the crack tip as a low-cycle fatigue micro-sample indirectly integrates environmental effects mainly through the use of a Manson-Coffin law.

The occurrence of hydrogen-assisted crack growth is associated to a typical change in the slope of the propagation curves which becomes close to 2 to 1 at low rates, and the transition from one regime (adsorption-assisted) to the other (hydrogen-assisted) often corresponds to a more or less well marked plateau range (Figs. 14 and 15).

The authors have proposed the following relationship based on a superposition principle to describe the propagation in an active moist environment

$$\frac{\mathrm{d}a}{\mathrm{d}N} = \frac{A}{D_1^*}\left(\frac{\Delta K_{\mathrm{eff}}}{\mu}\right)^4 + \frac{B}{\sigma\mu}(\Delta K_{\mathrm{eff}}^2 - \Delta K_{\mathrm{eff,th}}^2), \tag{2}$$

where $\Delta K_{\mathrm{eff,th}}$ denotes the threshold obtained under closure-free conditions, B is a dimensionless constant and σ a strength parameter.

The first term accounts for the adsorption-saturating regime previously described. The second one was subsequently added in an attempt to describe the hydrogen-assisted propagation regime. The $\Delta K_{\mathrm{eff}}^2$ dependence might be viewed as a coarse description of the dislocation dragging via the CTOD. $\Delta K_{\mathrm{eff,th}}$ would thus denote a threshold value of this sweep-in mechanism to enable the attainment of a critical hydrogen concentration at the crack tip. However, such a formulation for hydrogen-assisted propagation is still highly empirical. Problems arise from the lack of a sound understanding of what happens ahead of the crack tip. Some critical issues are required to be answered for a detailed knowledge to achieve this goal. Finally, the temperature dependence of these phenomena obviously constitutes a prime issue for investigation.

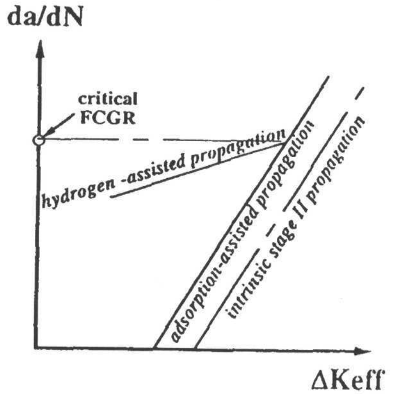

Fig. 14. Schematic illustration of environmentally-assisted stage II fatigue crack growth mechanisms.

5. Conclusion

In this overview of the influence of microstructure and environment on the fatigue crack propagation behaviour of metallic alloys some aspects have been emphasized:

– the homogeneity of the plastic deformation is a critical process influencing crack propagation. It depends on alloy composition, size and morphology of grains, phase distribution, size and coherence of precipitates;

– microstructure has little influence on the effective stage II propagation for a given based matrix metal, but has a high influence on crystallographic propagation (stage-I-like regime) which predominates in the near-threshold area;

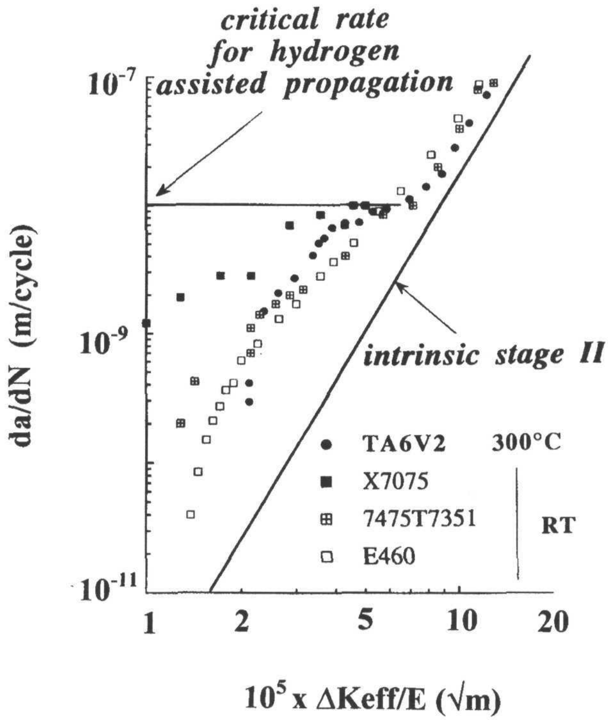

Fig. 15. Critical rate for enhanced near-threshold environmental effect.

– microstructure can strongly modify the closure contribution;

– ambient air and moist environments can strongly affect the propagation mechanisms. An important role of water vapour has been underlined. The behaviour in moist environments has been described by superimposing two distinct processes: adsorption of water vapour molecules which promotes the growth process without altering the base intrinsic mechanism of damage accumulation, and hydrogen-assisted propagation which is operative at rates below a critical range depending on several factors including test frequency;

– the water-vapour assistance favours the activation of multiple slip systems and hence promotes the stage II regime;

– three intrinsic crack propagation regimes have been clearly identified;

– constitutive laws are proposed to describe the intrinsic propagation and for water-vapour-assisted propagation.

REFERENCES

[1] CAZAUD, R.—POMEY, G.—RABBE, P.—JANSSEN, CH.: In: La fatigue des métaux. Paris, Dunod 1969.
[2] FINE, J.: In: ASM Materials Science Seminar. 1979, St. Louis, USA.
[3] FRANCOIS, D.: Advances in Fatigue Science and Technology. Eds.: Maura Branco, C. et al. Dordrecht, Kluwer Acad. Pub. 1989, p. 23.
[4] PETIT, J.—De FOUQUET, J.—HENAFF, G.: Handbook of Fatigue Crack Propagation in Metallic Structures. Ed.: Carpinterie, A. London, Elsevier Pub. *2.* 1994, p. 1159.
[5] HABERZ, K.—PIPPAN, R.—STÜWE, H. P.: In: Proceedings of Fatigue 93. *1.* Eds.: Bailon, J. P. and Dickson, J. I. EMAS pub. 1993, p. 525.
[6] SURESH, S.—RITCHIE, R. O.: Fatigue Crack Growth Threshold Concepts. Eds.: Davidson, D. et al. TMS AIME pub. 1984, p. 227.
[7] SURESH, S.: Metall. Trans. A., *16A*, 1985, p. 249.
[8] PETIT, J.: Fatigue Crack Growth Threshold Concepts. Eds.: Davidson, D. et al. TMS AIME pub. 1984, p. 3.
[9] SARRAZIN, C.—LESTERLIN, S.—PETIT, J.: ASTM STP 1296, in print.
[10] VANKATESWARA, K. T.—RITCHIE, R. O.: In: Report B.L. 30176. Center for Advanced Materials, Univ. of California 1991.
[11] MINAKAWA, K.—MATSUO, K. Y.—Mc EVILY, A. J.: Metall. Trans. A., *13A*, 1982, p. 439.
[12] LINDIGKEIT, J.—TERLINDE, G.—GYSLER, A.—LÜTJERING, G.: Acta Metall., *27*, 1979, p. 1717.
[13] KIRBY, B. R.—BEEVERS, C. J.: Fatigue Engng. Mater. Struct., *1*, *1979*, p. 203.
[14] TURNBULL, A.—de los RIOS, E. R.: Fatigue Fract. Engng. Mat. Struct., *18*, 1995, p. 1355.
[15] Mc CLINTOCK, F. A.: Fracture of Solids. Inter science pub. 1963, p. 65.
[16] RICE, J. P. : ASTM STP 416, 1965.
[17] WEERTMAN, J.: Int. J. Fract. Mech., *2*, 1966, p. 460.
[18] XU, Y. B.—WANG, L.—ZHANG, Y.—WANG, Z. G.—HU, Q. Z.: Metal Trans., *22A*, 1991, p. 723.
[19] HENAFF, G.—MARCHAL, K.—PETIT, J.: Acta Metall. Mater., *43*, 1995, p. 2931.
[20] LYNCH, S. P.: Acta Metall., *36*, 1988, p. 2639.